Desalination and Water Treatment
www.deswater.com

doi: 10.5004/dwt.2017.21418

90 (2017) 231–240
September

Phenol adsorption onto coffee waste – granular activated carbon: kinetics and equilibrium studies in aqueous solutions

María de la Luz Díaz de León-Garza, Eduardo Soto-Regalado*, Margarita Loredo-Cancino, Felipe de Jesús Cerino-Cordova, Refugio Bernardo García-Reyes, Nancy Elizabeth Dávila-Guzmán, José Ángel Loredo-Medrano

Facultad de Ciencias Químicas, Universidad Autónoma de Nuevo León, Av. Universidad S/N, Cd. Universitaria, San Nicolás de los Garza, NL 66455, México, Tel/Fax: + 52 8183294000; emails: eduardo.sotorg@uanl.edu.mx (E. Soto-Regalado), ml.diaz@hotmail.com (M.d.l.L. Díaz de León-Garza), margarita.loredocn@uanl.edu.mx (M. Loredo-Cancino), felipejccuanl@yahoo.com.mx (F.d.J. Cerino-Córdova), bernardogarciareyes@yahoo.com.mx (R.B. García-Reyes), nancy.davilagz@uanl.edu.mx (N.E. Dávila-Guzmán), jaloredom@hotmail.com (J.Á. Loredo-Medrano)

Received 14 February 2017; Accepted 4 September 2017

ABSTRACT

In this research, the production of granular activated carbon from coffee waste (CW) by chemical activation with zinc chloride was studied by using a 2^3 factorial design with the three responses (surface area, yield, and hardness) and studying three factors (the activation temperature, activation time, and impregnation ratio). The findings expose that after the experimental design, the highest response values were achieved at an activation temperature of 600°C, an activation time of 40 min, and an impregnation ratio of 1.5 g $ZnCl_2$ g^{-1} CW. At these conditions, the experimental tests produced a surface area of 1,279 m^2 g^{-1}. Batch studies of phenol adsorption onto coffee waste-activated carbon (CW-GAC) were performed at different solution pH, stirring speeds, and initial phenol concentrations. The maximum phenol adsorption capacity onto CW-GAC was 160.52 mg g^{-1} at pH 7. The adsorption kinetics was affected by stirring speed, the required time to achieve equilibrium decreased from 150 to 120 min when stirring speed varied from 200 to 400 min^{-1}. Film and intraparticle diffusion mechanisms controlled the adsorption of phenol onto CW-GAC. Finally, the porous material developed in this research is capable of sequestering phenol from aqueous solutions to a higher extent than similar lignocellulosic-based activated carbons.

Keywords: Adsorption; Coffee; Factorial experimental design; Granular activated carbon; Lignocellulosic waste

---

1. Introduction

Phenol and its derivatives are aromatic compounds present in wastewater from pharmaceutical, coal tar, plastics, leather, paints, steel, textiles, paper, insecticides, pesticides, phenolic resins, and oil refinery industries [1,2]. Phenol is toxic, mutagenic, and could cause diarrhoea, mouth sores, and dark urine in case of repeated oral exposure [3]. Furthermore, phenol represents a serious environmental problem due to its limited biodegradability; hence, it remains for long periods in soil, surface water, and even in groundwater where it interferes with natural, physical, chemical, and biological processes. Phenol is registered as priority pollutant by the US Environmental Protection Agency with a permissible limit of 0.1 mg L^{-1} in wastewater [4].

The activated carbon is a versatile adsorbent used in environmental remediation processes because of its high specific surface area and the possibility of incorporating functional groups on the adsorbent surface. However, recent studies

---

* Corresponding author.

have focused on the use of agro-industrial wastes as low-cost precursors for activated carbon production such as barley husks [5], wood [6], fruit stones [7], coconut shell [8], almond shells [9], bagasse sugar [10], rice husk [11], and coffee residue [12], among others. According to the U.S. Department of Agriculture, the worldwide coffee production in 2017/18 is forecast to be 9.540 × 10^9 kg [13]. The coffee beverage industry generates large quantities of spent coffee ground as a by-product, which represents serious environmental problems.

The manufacture of activated carbon consists of the pyrolysis of the precursor material and the development of its porous structure by physical or chemical activation. The chemical activation of the carbon involves heating the precursor material to temperatures ranging between 400°C and 900°C and the addition of activating agents such as KOH, K_2CO_3, NaOH, $ZnCl_2$, or H_3PO_4. To determine the efficiency of the chemical activation process, parameters such as yield, surface area, iodine number, energy and chemical consumption, among others, are commonly measured. These factors are affected by the manufacturing conditions, for instance temperature, activating agent impregnation ratio, and activation time. Thus, to explain the effect of the above-mentioned parameters on yield and surface area, some authors [14] have used an experimental design to select the adequate operational conditions to carry out the production of activated carbon.

The aim of this research was to evaluate the effect of the impregnation ratio of zinc chloride as the activating agent, temperature and time in the manufacturing of activated carbon from coffee waste (CW) on responses as surface area, yield, and hardness. In addition, the activated carbon produced at the best experimental conditions was tested to remove phenol from aqueous solution, assessing both the adsorption capacity and kinetic parameters.

2. Materials and methods

2.1. Precursor

CW was collected locally and used as a precursor of activated carbon. To remove soluble materials from the precursor, the CW was washed with boiling water until a non-colour solution was obtained. Then, CW was dried and stored in desiccator at room temperature for its further use.

2.2. Chemicals

The chemical substances used in this project were of analytical reagent grade. Phenol and zinc chloride were bought from Sigma-Aldrich, México and CTR, México respectively. Chemicals (KI, I_2, $Na_2S_2O_3.5H_2O$, KIO_3, and Na_2CO_3) and standard solutions (0.1 N NaOH, 0.1 N HCl, 0.1 N Na_2CO_3, and 0.1 N $NaHCO_3$) were obtained from DEQ, México. NaOH and NaCl were obtained from Merck, México. Concentrated HCl was obtained from PQM, México and high purity nitrogen was obtained from AOC, Mexico. Bi-distilled water for the solutions was obtained from a local company.

2.3. Preparation of granular activated carbon

Solutions of the chemical activating agent were prepared dissolving a known mass of $ZnCl_2$ in bi-distilled water to obtain a ratio of 1:10 (w:v). These solutions were used to impregnate the precursor (CW) at two weight ratios, as shown in Table 1. The impregnation process was conducted submerging CW in the $ZnCl_2$ solutions and stirring at boiling point for 6 h. Subsequently, the CW and the solutions were separated by filtration, after that impregnated CW was dried at 80°C for 24 h. Afterwards, a mass of 120 g of the impregnated precursor was placed into a horizontal rotary electric furnace (HTR 11/150, Carbolite) and heated under a nitrogen flow of 2 mL min^{-1}, at a heating rate of 6°C min^{-1} until reaching the selected activation temperatures (Table 1). Each sample was kept at these conditions during selected times according to the 2^3 factorial design showed in Table 1. The best conditions for the production of activated carbon from CW were determined studying the effect of three studied factors on three responses (surface area, yield, and hardness).

Analysis of variance (ANOVA) was carried out by using the Design-Expert software (version 7.0.0, Stat-Ease, Inc., USA), to determine the effects of factors on the studied responses (surface area, yield, and hardness). In order to evaluate the effect of the factor in the selected responses, a statistical model was built taking into account the significant factors.

The activated carbons (CW-GAC) obtained from each experimental run were washed using 0.1 N HCl solution to remove the remaining $ZnCl_2$ from the adsorbent material. Afterwards, the materials were washed several times until

Table 1
Experimental design and the physical characteristics (responses) analysed

Factors			Responses		
A (temperature, °C)	B (activation time, min)	C (impregnation ratio, g $ZnCl_2$ g^{-1} spent coffee ground)	Surface area (m^2 g^{-1})	Yield (%)	Hardness (%)
450	40	0.5	1,165.04	24.26	95.77
600	40	0.5	943.43	20.06	96.67
450	120	0.5	1,215.62	26.44	79.80
600	120	0.5	726.28	18.73	91.87
450	40	1.5	1,059.16	18.86	83.60
600	40	1.5	1,279.96	26.00	76.77
450	120	1.5	1,109.44	25.43	80.37
600	120	1.5	1,178.99	17.87	92.17

reaching a neutral pH in the washing solution. Finally, the CW-GAC were dried at 60°C during 12 h and stored for its further use in both equilibrium and kinetic adsorption experiments.

The CW-GAC yield is useful to determine the carbonisation efficiency, and it was calculated according to Eq. (1):

$$\text{CW}-\text{GAC Yield}=\left(m_{\text{GAC}}/m_{\text{precursor}}\right)\times 100 \tag{1}$$

where m_{GAC} (g) is the dry mass of CW-GAC, and $m_{\text{precursor}}$ (g) is the dry mass of CW.

Hardness is a measure of the resistance of solid matter, and this parameter is important in order to avoid abrasion and the loss of the adsorbent. This property was determined by the method reported by Ahmedna et al. [8] as follows: 3 g of CW-GAC (12/40 Tyler mesh) were placed in a 250 mL Erlenmeyer flask that contained 10 glass balls of 5 g each. The flask was continuously stirred at 200 min^{-1} in an orbital shaker (MaxQLabline 4000, Barnstead) for 15 min at room temperature. The resulting sample was sieved through a 40 Tyler mesh and the retained CW-GAC was weighed. Then, the hardness percentage was calculated as follows:

$$\%\ \text{Hardness}=\frac{\text{g carbon retained on 40 Tyler mesh}}{\text{3 g total sample}}\times 100 \tag{2}$$

2.4. Materials characterization

The adsorbent material was characterised to determine fixed carbon, volatile mater, ash, and moisture content. An elemental analysis was conducted to quantify C, H, N, and S by using an elemental analyser (2400 Series II, PerkinElmer, Mexico). Additionally, a proximate analysis was performed according to the ASTM Standard D3172 [15].

The pore size distribution and specific surface area are important properties of the adsorbent materials. In order to determine these properties, an ASAP 2020 (Micromeritics) analyser was used after out-gassing CW-GAC, by the adsorption/desorption isotherm of ultra-high purity nitrogen (99.999%) at –196°C and 32 different partial pressures (0.01–0.995), at 500 μm of Hg for 360 min. The obtained adsorption data were modelled by the BET equation.

In aqueous solution, an adsorbent acquires a positive or negative surface charge as a result of the interactions between the functional groups in the adsorbent and the ions present in solution. The net surface charge will be neutral when the amount of the positive and negative charges is equal (point of zero charge pH_{PZC}). The pH_{PZC} of CW-GAC was determined based on the Boehm titration method as follows: nine different volumes of 0.1 M NaOH or HCl were placed in 25 mL volumetric flasks and filled to the mark with 0.1 N NaCl. Then, 0.1 g of CW-GAC were added to the solutions and stirred continuously for 7 d at 25°C. The final pH was measured at the end of the experiment. Blank tests were simultaneously carried out without CW-GAC under the same conditions.

The identification and quantification of the functional groups on activated carbon is useful for understanding the interactions between the adsorbate and adsorbent. The surface functional groups were identified using an Fourier-transform infrared spectrometer (Spectrum One, PerkinElmer) and a scanning was recorded in the range of 4,000–650 cm^{-1}. The functional groups on the adsorbent surface were quantified by the Boehm titration method [16] as follows: a mass of 100 mg of CW-GAC was placed in 50 mL conical tubes containing 25 mL of 0.1 N NaOH, 0.1 N $NaHCO_3$, 0.1 N Na_2CO_3, or 0.1 N HCl. The vials were shaken for 7 d at 200 min^{-1} and 25°C. Subsequently, an aliquot of 10 mL of the supernatant was titrated with 0.1 N HCl or 0.1 N NaOH using phenolphthalein as an indicator. All experiments were performed in duplicate and the results are expressed in mEq of H^+ g^{-1} of the adsorbent.

2.5. Adsorption kinetic experiments

A rotating basket reactor [17] containing a known amount of CW-GAC was placed in a beaker with 1,000 mL of a 200 mg L^{-1} phenol solution, and stirred at predetermined speeds (200, 300, and 400 min^{-1}), 30°C and pH 7. The adsorption process was allowed to occur for 600 min, and aliquots were taken at pre-set time intervals. The phenol concentration in aliquots was determined by UV–Vis spectrophotometry at 270 nm. The adsorption capacity q_t (mg g^{-1}) was calculated by Eq. (3).

$$q_t=\frac{V\left(C_0-C_t\right)}{W} \tag{3}$$

where C_0 (mg L^{-1}) and C_t (mg L^{-1}) represent the initial concentration and concentration at any time, respectively. V (L) represents the volume of phenol solution, and W (g) is the mass of adsorbent.

The kinetic parameters were calculated using the mathematical expressions for pseudo-first-order, pseudo-second-order, and Weber and Morris models given by Eqs. (4)–(6), respectively:

$$q_t=q_e\left(1-e^{-k_1 t}\right) \tag{4}$$

$$q_t=\frac{(q_e^2 k_2 t)}{(1+q_e k_2 t)} \tag{5}$$

$$q_t=k_p t^{0.5}+I \tag{6}$$

where q_t (mg g^{-1}) is the quantity of adsorbate adsorbed at time t (s), q_e (mg g^{-1}) is the adsorption capacity at equilibrium, and k_1, k_2, and k_p are the kinetic parameters of Eqs. (4)–(6), respectively.

2.6. Equilibrium adsorption experiments

Before the equilibrium adsorption experiments, the CW-GAC was hydrated with bi-distilled water to minimise the formation of air bubbles inside the solid. A quantity of CW-GAC (12.5, 25, and 50 mg) was placed in 50 mL conical tubes containing 25 mL of aqueous solutions of known phenol concentrations (5, 10, 20, 30, 40, 50, 60, 80, 100, 120, 160, and 200 mg L^{-1}). Conical tubes containing the phenol solutions and the CW-GAC were stirred continuously for 7 d in an orbital shaker (Barnstead MAX Q 4000) at 200 $\min^{-1}$ and room temperature. The initial pH of the solution was 7, and it was not controlled during the experiment. Blank tests were simultaneously performed without activated carbon under the same experimental conditions. Once the equilibrium was achieved, the mixture was filtered and the filtrate was analysed by spectrophotometry at 270 nm, all the experimental runs were performed in triplicate.

At equilibrium, there is a fixed mass distribution of the adsorbate between the liquid and solid phases. For describing this arrangement, the quantity of adsorbed solute per unit mass of adsorbent (q_e) is usually expressed as a function of the residual equilibrium concentration (C_e) of the solute remaining in the liquid phase. These values of q_e and C_e can be related by an equation referred as adsorption isotherm. The isotherms are useful for describing the adsorption capacity and to perform the assessment in the feasibility of the process for a particular application. The most commonly reported isotherm equations in literature for several systems are the Langmuir [18], Freundlich [19], and Redlich–Peterson [20] models. These isotherm models were compared with predict equilibrium adsorption data. Their expressions are given in Eqs. (7)–(9), respectively:

$$q_e = \frac{q_m b C_e}{1 + bC_e} \tag{7}$$

$$q_e = KC_e^{1/n} \tag{8}$$

$$q_e = \frac{K_{RP} C_e}{1 + \alpha C_e^{\beta}} \tag{9}$$

where q_e (mg g^{-1}) is the quantity of adsorbate adsorbed at equilibrium, q_m (mg g^{-1}) is the maximum adsorption capacity, C_e (mg L^{-1}) is the concentration at equilibrium, and K, K_{RP}, n, α, b, and β are parameters of each isotherm models.

2.7. Desorption experiments

Previous to phenol desorption experiments, the CW-GAC was used as adsorbent of phenol from aqueous solution as described in section 2.6. After that, the CW-GAC was separated by filtration and slightly washed with deionised water to remove the residual phenol solution. Then, phenol desorption experiments were carried out as follows: 0.5 g of phenol-loaded CW-GAC were place into 250 mL glass flasks containing 0.5 L of 0.1 N NaOH solution. This suspension was stirred at 200 $\min^{-1}$ and room temperature for 4 h. Finally, aliquots were taken from the liquid solution in order to determine phenol concentration by UV–Vis spectrophotometry. Four adsorption–desorption cycles were conducted to evaluate the reusability of the CW-GAC during the removal of phenol from aqueous solutions.

2.7. Error analysis

The isotherm and kinetic model parameters were determined using the Solver function of Microsoft Excel®, with the average relative error (ARE) as an error function to determine the accuracy of the regression. This error function attempted to minimise the fractional error distribution across the complete studied range. The ARE was calculated according to Eq. (10):

$$\text{ARE} = \left(\frac{1}{N} \sum_{i=1}^{N} \left| \frac{q_{\text{exp}} - q_{\text{calc}}}{q_{\text{exp}}} \right| \right) \times 100 \tag{10}$$

where N is the number of experimental points, and q_{exp} and q_{calc} represent the experimental and predicted phenol adsorption capacity, respectively.

3. Results and discussion

3.1. Precursor properties

Proximate analysis of the CW revealed that this waste contains 85.44% volatile matter, 13.4% of fixed carbon, and 1.4% ash, besides the elemental analysis showed that the precursor contains 44.49% carbon, 9.98% hydrogen, 1.95% nitrogen, 1.23% sulphur, and 42.35% oxygen (estimated by difference). Similar values have been reported for other lignocellulosic residues used as activated carbon precursor [7,21,22]. Therefore, CW can be considered an interesting alternative to produce activated carbon, since it has a high content of volatile matter and low content of ash as well as fixed carbon.

3.2. Statistical analysis

Table 1 shows the conditions and the experimental results for the production of CW-GAC. After discarding the non-significant terms, the ANOVA data for the coded model of the surface area and yield are showed in Tables 2 and 3, respectively. Based on the ANOVA data for the surface area, the most significant individual factor was the impregnation ratio, and the most significant double interaction was between the temperature and the impregnation ratio (Eq. (11)). Similar results were reported by Loredo-Cancino et al. [14] for the activated carbon produced from barley husks. Additionally, the activation time did not have a significant effect on the surface area, and, therefore, this independent factor was not included in final coded model (Eq. (11)):

$$\text{Surface area} = 1{,}084.73 + 72.13\text{C} + 125.15\text{AC} \tag{11}$$

Based on the ANOVA data for the yield response (Table 3), the most significant individual factor was the temperature,

Table 2
The analysis of variance data for surface area determined from a 2^3 experimental design

Source	Sum of squares	Degree of freedom	Mean square	F-value	*p*-value
Model	1.6692×10^5	2	8.3383×10^4	7.8168	0.0288
C	4.1621×10^4	1	4.1621×10^4	3.8982	0.1051
AC	1.2530×10^5	1	1.2530×10^5	11.7355	0.0187
Residual	5.3384×10^4	5	1.0677×10^4		
Total	2.2030×10^5	7			

Table 3
The analysis of variance data for yield determined from a 2^3 experimental design

Source	Sum of squares	Degree of freedom	Mean square	F-value	*p*-value
Model	92.61	4	23.15	68.76	0.0028
A	19.00	1	19.00	56.44	0.0049
AB	41.45	1	41.45	123.10	0.0016
AC	16.50	1	16.50	49.01	0.0060
ABC	15.65	1	15.65	46.48	0.0065
Residual	1.01	3	0.34		
Total	93.62	7			

Table 4
The analysis of variance data for hardness determined from a 2^3 experimental design

Source	Sum of squares	Degree of freedom	Mean square	F-value	*p*-value
Model	425.79	6	70.97	10.20	0.2352
A	40.23	1	40.23	5.78	0.2509
B	9.25	1	9.25	1.33	0.4549
C	121.68	1	121.68	17.49	0.1494
AB	111.01	1	111.01	15.96	0.1562
AC	8.00	1	8.00	1.15	0.4778
BC	135.63	1	135.63	19.50	0.1418
Residual	6.96	1	6.96		
Total	432.75	7			

the most significant double interactions were between the temperature and the time, as well as temperature and the impregnation ratio, and the most significant triple interaction was between temperature, time, and impregnation ratio (Eq. (12)). The activation time did not show a significant effect on the yield response:

$$\text{Yield} = 22.21 - 1.54A - 2.28AB + 1.44AC - 1.40ABC \qquad (12)$$

The ANOVA data for the coded model of the hardness response indicated that neither temperature, time, nor impregnation ratio attained a significant effect in hardness, as shown in Table 4.

The mathematical model for the surface area (Eq. (11)) and yield (Eq. (12)) was used to build response surfaces and contour plots. For the above-mentioned purposes, an activation time of 40 min was selected because this factor was not significant for the studied responses (Fig. 1). Moreover, for practical and economic reasons, it is desirable to choose the lowest activation time in the studied range to reduce the energy consumption in the pyrolysis process. It is important to mention that the model includes interaction between factors and, therefore, the response surface is a twisted plane. It is desirable to operate the CW-GAC production process to achieve the highest surface area and yield. Fig. 1 shows that if time is at the low level, the maximum surface area and yield occurred at 600°C and an impregnation ratio of 1.5 g $ZnCl_2$ g^{-1} CW. The effect of impregnation ratio on the response could be explained as follows, the $ZnCl_2$ assumes a role as a dehydration agent during activation, inhibiting the formation of tars and other liquids that could clog up the pores of the carbons. For this reason, an increase in the impregnation ratio enhances the movement of the volatiles through the pores and, consequently, causes an increase in the surface area [14].

3.3. Physical and chemical properties of coffee-waste ground granular activated carbon

Table 5 shows the physical and the textural properties of CW-GAC produced at 600°C, 40 min, and an impregnation ratio of 1.5. The CW-GAC has a surface area of 1,280 m^2 g^{-1}, which is similar to other lignocellulosic granular [1,7,9] and powdered [2,5,10,14,22] activated carbons.

The obtained adsorbent (CW-GAC) was characterised by potentiometric titrations in order to determine the surface charge distribution and the concentration of active sites. The concentration of acidic sites (3.00 mEq g^{-1}) is greater than that of basic sites (0.75 mEq g^{-1}), hence, the surface is acidic predominantly. The different types of acidic sites were also determined, and it was found that their concentrations were 1.75 mEq g^{-1} phenolic groups, 0.75 mEq g^{-1} lactonic groups, and 0.5–0.75 mEq g^{-1} carboxylic acid groups.

The adsorbent net surface charge distribution is a function of the type and quantity of functional groups, and the solution pH. At solution pH values higher than the pH_{PZC}, the adsorbent surface acquires a negative net charge, while the adsorbents surface presented a positive net charge at pH values lower than pH_{PZC}. The determination of the surface charge distribution on the activated carbon helps to explain the mechanism of adsorption of ionised pollutants [23]. The pH_{PZC} value of CW-GAC was determined to be 3.9, indicating that it is acidic. The high content of acidic functional groups leads to a pH_{PZC} lower than 7 and, for that reason, this material seems to be helpful for adsorbing heavy metals, basic dyes, and other positively charged species from aqueous solutions, a similar behaviour has been reported by other authors for activated carbons [24–27]. The presence of phenolic and carboxylic acid groups was confirmed by FTIR analysis (Fig. 2).

3.4. Effect of pH

The chemical speciation of an adsorbate and the surface charge of an adsorbent depend on the pH of solution. Thus, in order to evaluate the effect of the pH on the adsorption capacity, three pH conditions were evaluated (pH 3, 6, and 11). Fig. 3 depicts the effect of pH on the adsorption capacity of phenol onto CW-GAC, it can be observed an increase of 7% with the augmentation of the pH from 3 to 6. However, if the solution pH increased from 6 to 11, the adsorption capacity decreased by 27%. The decrease in the adsorption capacity at basic conditions could be explained taking into account the speciation diagram of the phenol (pKa = 9.89). At pH 11, 90% of the phenol is present as phenolate (i.e., negative-charged species), meanwhile the CW-GAC surface charge is predominantly negative according to its pH_{PZC} (3.9). Therefore, electrostatic repulsion can occur between the phenolate ions and the ionised acid groups on the adsorbent surface.

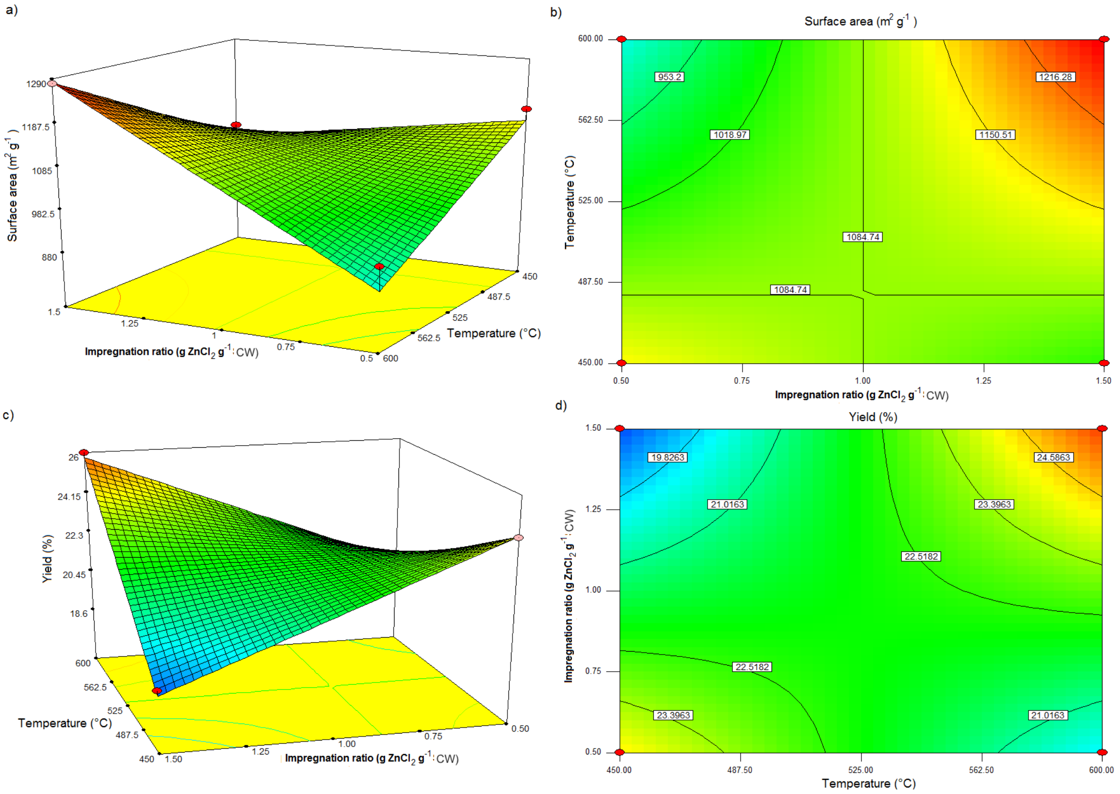

Fig. 1. The response surface and corresponding contour plot for the surface area (a and b) and the yield (c and d).

Table 5
Comparison of the CW-GAC production conditions, properties, and phenol adsorption capacity with literature data

Precursor (RI, Tact, tact)	Yield (%)	Surface area BET ($m^2 g^{-1}$)	Total pore volume ($cm^3 g^{-1}$)	Average pore diameter (Å)	Initial phenol concentration (mg L^{-1})	Adsorption capacity (mg g^{-1})	Solution pH	Reference
Coffee waste (1.5, 600°C, 40 min)	26.00	1,280	0.77	33	200	160.52	7	This research
Barley husk (1.5, 600°C, 40 min)	48.48	811	0.263	–	1,000	132.9	7	Loredo-Cancino et al. [5,14]
Rice husk (4.2, 900°C, 60 min)	37.69	439	0.387	35.28	300	62.1	2.7	Kennedy et al. [1]
Olive husk (4, 800°C, 60 min)	–	1,880	1.1114	22.16	–	–	–	Michailof et al. [2]
Coconut shells (2, 800°C, 60 min)	99.35	380	0.36	–	94	38.82	2 ± 0.2	Singh et al. [10]
Hazelnut shell (750°C, 600 min)	37	793	–	–	–	145	–	Aygün et al. [7]
Almond shell (450°C, 60 min)	37	1,340	–	–	–	–	–	Bansode et al. [9]
Date stones (0.5, 700°C, 180 min)	–	951	–	–	–	–	–	Alhamed [28]
Sugar cane bagasse (0.25, 500°C, 60 min)	24.87	1,611	1.233	30.6	–	–	–	Liou [22]

Note: RI, ratio of precursor impregnation/activating agent (w/w); Tact, activation temperature (°C); tact, activation time (min).

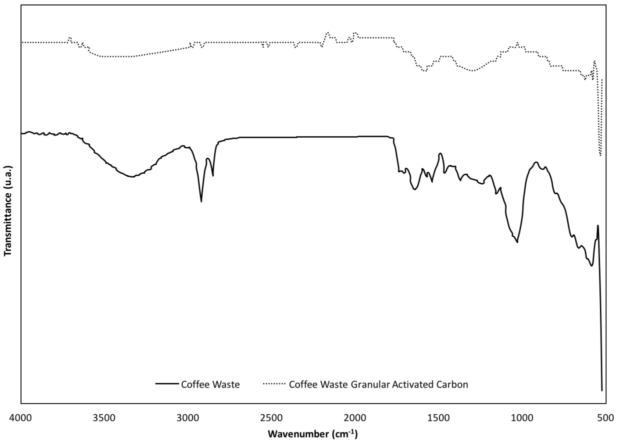

Fig. 2. FTIR spectra for CW-GAC produced at 600°C, 40 min of activation time, and an impregnation ratio of 1.5 g $ZnCl_2$ g^{-1} of CW.

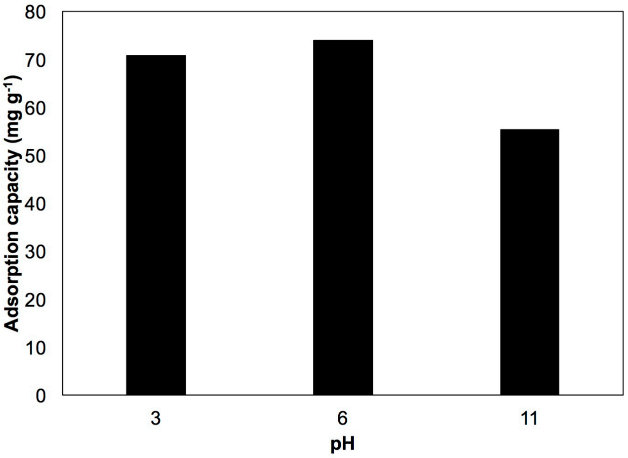

Fig. 3. The effect of pH on the phenol adsorption capacity onto CW-GAC (q_e, mg g^{-1}) at initial phenol concentration of 250 mg L^{-1}.

3.5. Kinetic studies

In order to determine the time to reach equilibrium and to assess the effect of stirring speed on the uptake rate of phenol, adsorption kinetic experiments were performed at different stirring speeds (200, 300, and 400 min^{-1}) at 30°C, pH 7, and an initial phenol concentration of 200 mg L^{-1}. Figs. 4(a) and (b) show the kinetics of phenol adsorption onto CW-GAC under different stirring speeds, and the predicted data by pseudo-first-order and pseudo-second-order models. As shown in Fig. 4, the time to reach equilibrium decreased when the stirring speed was increased from 200 to 400 min^{-1}. This behaviour could be attributed to the reduction of the boundary layer surrounding the adsorbent particle, hence, phenol molecules are transported at a faster rate to the external surface of the adsorbent.

The experimental kinetic data were used to estimate the adsorption kinetic parameters for the kinetic models, and these parameters are shown in Table 6. Parameters of kinetic models were determined by least square method using Solver tool of Excel®, and the ARE was used to determine the best fit for the studied models. For all stirring speeds, the pseudo-second-order model predicted the experimental kinetic data better than the pseudo-first-order model based on the low ARE value. Additionally, the rate constant (k_2) increases 1.98 times with the increment of the stirring speed from 200 to 400 min^{-1}, indicating a faster adsorption at high stirring speeds.

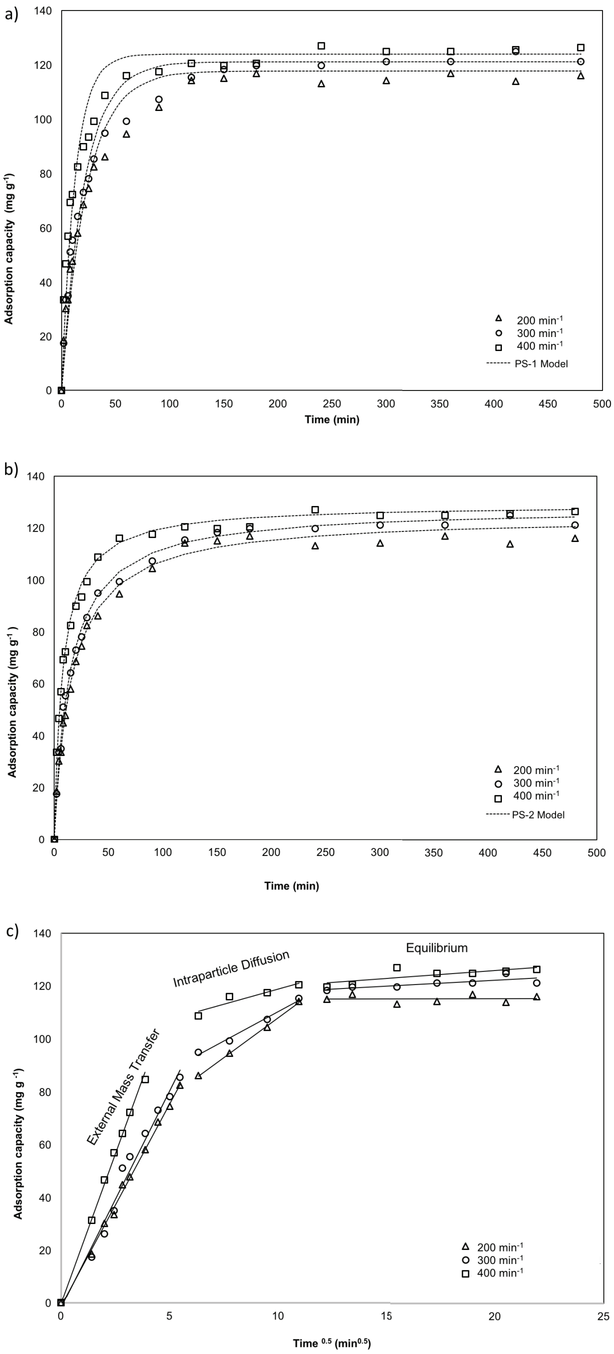

Fig. 4. Adsorption kinetics of phenol onto CW-GAC using different stirring speeds (pH 7, 30°C, and initial phenol concentration of 200 mg L^{-1}). Symbols represent experimental data and lines represent the predicted values by (a) pseudo-first-order model, (b) pseudo-second-order model, and (c) intraparticle diffusion model.

The intraparticle diffusion model was employed in order to determine the rate-controlling step (Fig. 4(c)). According to the Weber and Morris model, a straight line should be obtained if the intraparticle diffusion is involved and this line should pass the origin when is the rate-controlling step [29]. As can be seen in Fig. 4(c), the plot of q vs. $t^{1/2}$ shows multi-linearity suggesting that more than one diffusion step occurs in the adsorption process. The first linear section is related to the film diffusion, the second linear section corresponds to the intraparticle diffusion and the third section corresponds to the final stage of equilibrium where intraparticle diffusion begins to decrease due to the low concentration of the adsorbate in the solution and the reduced available active sites on the adsorbent surface [30]. Additionally, the kinetic parameter of the Weber and Morris model, K_p, was estimated for the first linear section showing an increase from 15 to 22.5 mg g^{-1} min$^{-0.5}$ with the increment of the stirring speed from 200 to 400 min^{-1}, respectively (Table 7). This behaviour is in agreement with the results obtained with the pseudo-first-order and pseudo-second-order models. Furthermore, it can be observed that the first linear section passes through the origin, suggesting that the intraparticle diffusion is the rate-controlling step.

3.6. Equilibrium adsorption experiments

The adsorption experiments at equilibrium are very important for the design of adsorption batch systems, and also to compare the performance of the adsorbents. A number of isotherms models are commonly used, for example: Langmuir [18], Freundlich [19], and Redlich–Peterson [20], among others. Table 8 shows the parameters of these isotherm models obtained from experimental data based on the ARE. The equilibrium adsorption data of phenol onto CW-GAC at adsorbent dosage of 1 g L^{-1} were satisfactorily predicted with the Redlich–Peterson isotherm model (ARE = 24.33). Fig. 5 shows the adsorption isotherm of phenol on CW-GAC and the predicted data from isotherm models. The maximum experimental adsorption capacity determined for phenol onto CW-GAC is comparable with or higher than those reported for activated carbon produced from other lignocellulosic precursors (Table 5).

3.7. Reusability of CW-GAC

From an economic point of view, adsorbent regeneration plays a key role in the removal of pollutants from aqueous solutions by adsorption processes. To regenerate CW-GAC, four adsorption/desorption cycles were carried out using sodium hydroxide as an eluent. Fig. 6 shows that phenol adsorption capacity approximately decreased 11% after the fourth adsorption cycle, whereas desorption capacity decreased from 78% to 56% in the first and fourth desorption cycle, respectively. Reduction in the phenol adsorption capacity could be attributed to the less available active sites

Table 6
Comparison of the pseudo-first-order and pseudo-second-order kinetic models for the phenol adsorption onto CW-GAC at different stirring speeds

Stirring speed (min^{-1})	Adsorption kinetic model					
	Pseudo–first-order			Pseudo-second-order		
	k_1 (min^{-1})	q_e (mg g^{-1})	ARE (%)	k_2 (g mg^{-1} min^{-1})	q_e (mg g^{-1})	ARE (%)
200	0.0431	117.64	8.12	5.005×10^{-4}	124.6	3.05
300	0.0476	121.13	10.42	5.454×10^{-4}	127.9	3.86
400	0.0804	123.92	9.64	9.948×10^{-4}	129.18	4.10

Table 7
Fitting parameters for intraparticle diffusion model for phenol adsorption onto CW-GAC at different stirring speeds

Stirring speed (min^{-1})	Adsorption kinetic model					
	First linear part of the curve			Second linear part of the curve		
	k_p (mg g^{-1} min$^{-0.5}$)	I (mg g^{-1})	ARE (%)	k_p (mg g^{-1} min$^{-0.5}$)	I (mg g^{-1})	ARE (%)
200	15.01	0.00	4.22	5.54	51.65	0.36
300	16.10	0.00	11.44	5.05	60.07	1.75
400	22.57	0.00	2.18	8.14	54.42	1.48

Table 8
Isotherm parameters estimated from experimental data of phenol adsorption onto CW-GAC

Langmuir				Freundlich				Redlich–Peterson				
q_{max}	b	*ARE (%)	R^2	K	n	*ARE (%)	R^2	K_{RP}	α_{RP}	β	*ARE (%)	R^2
160.52	0.07	26.77	0.84	7.13	1.39	40.43	0.82	8.94	0.04	1.37	24.33	0.94

*ARE values correspond to non-linear form of isotherm equations, and R^2 to linear form of isotherm equations. All isotherm parameters were estimated by the non-linear method.

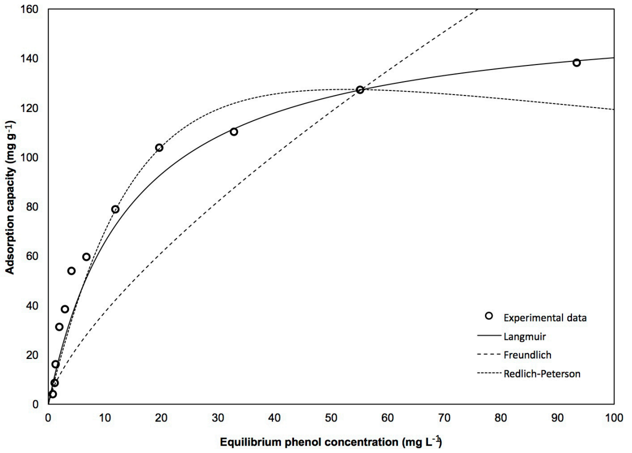

Fig. 5. The adsorption isotherm of phenol onto CW-GAC at pH 7 and 1.0 g L^{-1}. Symbols represent the experimental data and the lines indicate the isotherm models prediction.

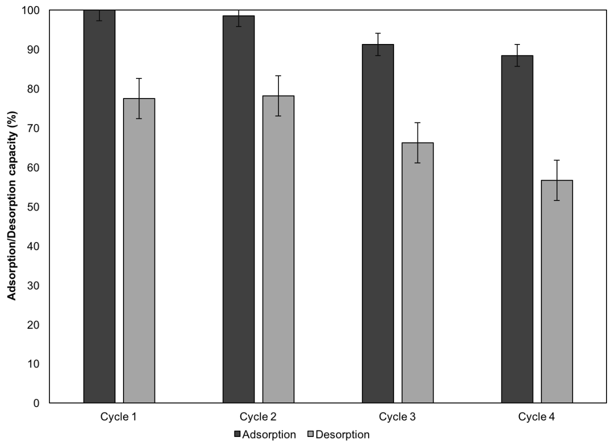

Fig. 6. Adsorption and desorption cycles of phenol onto CW-GAC with 0.1 N NaOH solution as the regenerating agent.

of the adsorbent as a consequence of the incomplete phenol desorption in previous cycles.

It is well known that desorption of phenol is a challenging process because of the low desorption efficiency. In this research, it was possible to achieve phenol desorption efficiencies higher than those reported for commercial activated carbon (61%) [31], groundnut shell adsorbent (40%) [32], and granular activated carbon (5.43%) [33]. These results clearly confirm the reusability of the CW-GAC for the removal of phenol from aqueous solutions.

4. Concluding remarks

This study demonstrates that CW can be used as a promising precursor to manufacture activated carbon and this adsorbent can be used for the removal of phenol from aqueous solutions. The obtained adsorbent at the optimal conditions (600°C, 40 min of activation, and an impregnation ratio of 1.5 g $ZnCl_2$ g^{-1} of CW) achieves a high surface area (1,280 m^2 g^{-1}) and acceptable hardness (76%–96%). The surface characterization indicates that adsorbent is acidic (pH_{PZC} = 3.9) and this characteristic implies that CW-GAC may be used as adsorbent of positively-charged species from aqueous solutions. The adsorption experiments showed that the removal of phenol by CW-GAC is effective at pH 6, and Redlich–Peterson isotherm adequately predicted the equilibrium adsorption data. The maximum adsorption capacity of phenol onto CW-GAC (160.52 mg g^{-1}) was comparable or higher than the values reported for lignocellulosic-based activated carbons. Adsorption kinetics of phenol on CW-GAC is predicted better with the pseudo-second-order model than the pseudo-first-order model, and the adsorption equilibrium is achieved in less than 150 min in all studied scenarios. Adsorption of phenol on CW-GAC is controlled by both film and intraparticle diffusion mechanisms since two remarked slopes are shown on the graph based on the Weber and Morris model. Desorption studies shows that recovery of phenol and regeneration of adsorbent are possible at least during four adsorption/desorption cycles.

Acknowledgements

This work was supported by the Facultad de Ciencias Químicas de la Universidad Autónoma de Nuevo León and CONACYT (Grant number 484808). The authors thank Gregorio Rosas-Sosa for providing assistance with elemental and proximal analysis.

Conflict of interest

The authors have declared no conflict of interest.

References

[1] L.J. Kennedy, J.J. Vijaya, K. Kayalvizhi, G. Sekaran, Adsorption of phenol from aqueous solutions using mesoporous carbon prepared by two-stage process, Chem. Eng. J., 132 (2007) 279–287.

[2] C. Michailof, G.G. Stavropoulos, C. Panayiotou, Enhanced adsorption of phenolic compounds, commonly encountered in olive mill wastewaters, on olive husk derived activated carbons, Bioresour. Technol., 99 (2008) 6400–6408.

[3] R.M. Bruce, J. Santodonato, M.W. Neal, Summary review of the health effects associated with phenol: health issue assessment, Toxicol. Ind. Health, 3 (1987) 535–568.

[4] US Environmental Protection Agency, Technical Support Document for Water Quality-based Toxics Control [Internet], 1985, Available at: http://www3.epa.gov/npdes/pubs/owm0264.pdf.

[5] M. Loredo-Cancino, E. Soto-Regalado, R.B. García-Reyes, F.J. Cerino-Córdova, M.T. Garza-González, M.M. Alcalá-Rodríguez, Adsorption and desorption of phenol onto barley husk-activated carbon in an airlift reactor, Desal. Wat. Treat., 57 (2014) 1–16.

[6] N. Tancredi, N. Medero, F. Möller, J. Píriz, C. Plada, T. Cordero, Phenol adsorption onto powdered and granular activated carbon prepared from Eucalyptus wood, J. Colloid Interface Sci., 279 (2004) 357–363.

[7] A. Aygün, S. Yenisoy-Karakaş, I. Duman, Production of granular activated carbon from fruit stones and nutshells and evaluation of their physical, chemical and adsorption properties, Micropor. Mesopor. Mater., 66 (2003) 189–195.

[8] M. Ahmedna, W. Marshall, R. Rao, Production of granular activated carbons from select agricultural by-products and evaluation of their physical, chemical and adsorption properties, Bioresour. Technol., 71 (2000) 113–123.

[9] R.R. Bansode, J.N. Losso, W.E. Marshall, R.M. Rao, R.J. Portier, Adsorption of volatile organic compounds by pecan shell- and almond shell-based granular activated carbons, Bioresour. Technol., 90 (2003) 175–184.

[10] K.P. Singh, A. Malik, S. Sinha, P. Ojha, Liquid-phase adsorption of phenols using activated carbons derived from agricultural waste material, J. Hazard. Mater., 150 (2008) 626–641.

[11] Y. Chen, Y. Zhu, Z. Wang, Y. Li, L. Wang, L. Ding, Application studies of activated carbon derived from rice husks produced by chemical-thermal process – a review, Adv. Colloid Interface Sci., 163 (2011) 39–52.

[12] M. Zahoor, Removal of crystal violet from water by adsorbent prepared from Turkish coffee residue, Tenside Surfactants Deterg., 49 (2012) 107–113.

[13] US Department of Agriculture, Coffee: World Markets and Trade [Internet], USDA, 2017, Available at: https://apps.fas.usda.gov/psdonline/circulars/coffee.pdf

[14] M. Loredo-Cancino, E. Soto-Regalado, F.J. Cerino-Córdova, R.B. García-Reyes, A.M. García-León, M.T. Garza-González, Determining optimal conditions to produce activated carbon from barley husks using single or dual optimization, J. Environ. Manage., 125 (2013) 117–125.

[15] ASTM International, Standard Practice for Proximate Analysis of Coal and Coke, West Conshohocken, PA, Standard No. ASTM D3172 – 13, 2007.

[16] H.P. Bohem, Chemical Identification of Surface Groups, D.D. Eley, H. Pines, P.B. Weisz, Eds., Advances in Catalysis, Academic Press, 1966, pp. 179–274.

[17] R.B. Garcia-Reyes, J.R. Rangel-Mendez, Adsorption kinetics of chromium(III) ions on agro-waste materials, Bioresour. Technol., 101 (2010) 8099–8108.

[18] I. Langmuir, The adsorption of gases on plane surfaces of glass, mica and platinum, J. Am. Chem. Soc., 40 (1918) 1361–1403.

[19] H. Freundlich, Über die Adsorption in Lösungen [adsorption in solution], Wilhelm Engelmann, Leipzig, 1906, German.

[20] O. Redlich, D.L. Peterson, A useful adsorption isotherm, J. Phys. Chem., 63 (1959) 1024.

[21] S.I. Mussatto, E.M.S. Machado, S. Martins, J.A. Teixeira, Production, composition, and application of coffee and its industrial residues, Food Bioprocess Technol., 4 (2011) 661–672.

[22] T.H. Liou, Development of mesoporous structure and high adsorption capacity of biomass-based activated carbon by phosphoric acid and zinc chloride activation, Chem. Eng. J., 158 (2010) 129–142.

[23] R. Leyva Ramos, Chapter V: Importancia y aplicaciones de la adsorción en fase líquida [Importance and applications of liquid phase adsorption], In: J.C. Moreno-Piraján, Ed., Sólidos Porosos: Preparación, Caracterización y Aplicaciones [Porous solids: preparation, characterization and applications], Ediciones Uniandes, 2007, pp. 155–207. Spanish.

[24] P.E. Diaz-Flores, R. Leyva-Ramos, R.M. Guerrero-Coronado, J. Mendoza-Barron, Adsorption of pentachlorophenol from aqueous solution onto activated carbon fiber, Ind. Eng. Chem. Res., 45 (2006) 330–336.

[25] B.M. Babic, S.K. Milonjic, M.J. Polovina, B.V. Kaludierovic, Point of zero charge and intrinsic equilibrium constants of activated carbon cloth, Carbon, 37 (1999) 477–481.

[26] D. Minguang, The effect of zeta potential of activated carbon on the adsorption of dyes from aqueous solution, J. Colloid Interface Sci., 164 (1994) 223–228.

[27] J.W. Shim, S.J. Park, S.K. Ryu, Effect of modification with HNO_3 and NaOH on metal adsorption by pitch-based activated carbon fibers, Carbon, 39 (2001) 1635–1642.

[28] Y. A. Alhamed, Adsorption kinetics and performance of packed bed adsorber for phenol removal using activated carbon from dates' stones, J. Hazard. Mater., 170 (2009) 763–770.

[29] W.J. Weber, J.C. Morris, Kinetics of adsorption on carbon from solution, J. Sanit. Eng. Div. Am. Soc. Civ. Eng., 89 (1963) 31–59.

[30] F.C. Wu, R.L. Tseng, R.S. Juang, Initial behavior of intraparticle diffusion model used in the description of adsorption kinetics, Chem. Eng. J., 153 (2009) 1–8.

[31] B. Ozkaya, Adsorption and desorption of phenol on activated carbon and a comparison of isotherm models, J. Hazard. Mater., 129 (2006) 158–163.

[32] S.J. Kulkarni, S. Gadgebaba, J.P. Kaware, Desorption studies for low cost adsorbents, Int. J. Chem. Stud., 3 (2015) 38–41.

[33] S. Suresh, V. Srivastava, I. Mishra, Studies of adsorption kinetics and regeneration of aniline, phenol, 4-chlorophenol and 4-nitrophenol by activated carbon, Chem. Ind. Chem. Eng. Q., 19 (2013) 195–212.